Molecular Vision 2021; 27:117-124 <http://www.molvis.org/molvis/v27/117>
Received 29 June 2020 | Accepted 29 March 2021 | Published 31 March 2021

Use of three-dimensional printing for adapting and optimizing smartphone ophthalmoscopy to existing SD-OCT instrumentation for rodent and teleost ocular research

James McDonald,[1] Hélène Paradis,[1] Michael Bartellas,[2] Robert L. Gendron[1]

[1]Division of BioMedical Sciences, Faculty of Medicine, Memorial University of Newfoundland, St. John's, N, Canada;
[2]Department of Otolaryngology, Faculty of Medicine, University of Ottawa, Ottawa, Ontario, Canada

Use of animal models for human vision research is now pervasive. To address a range of technical challenges, laboratories either modify existing equipment or purchase products that are purpose designed. Three-dimensional (3D) printing technology now allows the do-it-yourself capability to invent, innovate, and manufacture for a specific purpose. Ophthalmic imaging is often used with a range of other sophisticated experimental retinal imaging techniques, such as spectral domain optical coherence tomography (SD-OCT). The handheld smartphone camera and cost-effective, readily available professional-quality apps now allow accessible high-definition video ophthalmic image recording. However, to our knowledge, there are few reports of adapting smartphone ophthalmic imaging to existing experimental SD-OCT imaging instrumentation. This would offer better accuracy, reproducibility, and most importantly, precision. The objective of the present study was to use 3D printing to enhance the functionality and precision of existing SD-OCT instrumentation and smartphone-based ophthalmic imaging through construction of a custom 3D-printed assembly. The assembly can be controlled either manually or by the highly precise rodent stage of the SD-OCT instrument. Using this technical approach, 3D printing facilitated a novel methodology for high-quality ophthalmic imaging with low cost and ease of production either manually or by enhancing existing SD-OCT instrumentation.

Animal modeling of eye biology and new technologies: The utility of the genetically engineered mouse as an experimental model for human research is widely accepted [1]. Recently, we presented the marine teleost lumpfish, *Cyclopterus Lumpus* L., as a new model for ocular research and successfully performed spectral domain optical coherence tomography (SD-OCT) on these animals [2]. Although SD-OCT has been applied to zebrafish eye in several studies [3-5], this species is a freshwater teleost, and there have been, to our knowledge, no other reports of any type of ophthalmic imaging of marine teleosts.

To facilitate research in animal models, laboratories must either modify existing equipment or purchase products that are specifically designed for a purpose. With the recent increase in popularity of rapid prototyping, modifying equipment has become easier than ever. Universal access to free modeling software, online three-dimensional (3D) printing services, and low-cost desktop 3D printers have also made rapid prototyping extremely affordable. This technology has created an unprecedented era in which virtually everyone has the capability to invent, innovate, and manufacture for a specific purpose.

Three-dimensional printing: In the 1980s, additive manufacturing was introduced. This process involves fusing consecutive, two-dimensional layers of material until a 3D structure is produced [6]. As objects are produced using only the required amount of material, greater efficiency is achieved through reducing waste and cost. Today, this type of additive manufacturing is colloquially known as 3D printing, and it has established a key role in mainstream technology. A considerable amount of progress has been made in this field, and the machinery has become more affordable than ever. Even without owning printers, designers have access to affordable printing services through online communities that can connect designers to local facilities.

New approaches to ophthalmoscopy: Ophthalmic imaging approaches are now broadly adapted from retinal imaging methodologies based on the ophthalmoscope invented in 1851 by Hermann von Helmholtz. Fundus imaging using ophthalmic imaging approaches remains a simple but state-of-the-art retinal imaging methodology used in ophthalmology clinics worldwide. Ophthalmic imaging not only remains a standard diagnostic tool for retinal disease but also is useful in rapidly and noninvasively detecting signs of systemic diseases, such as diabetes. Ophthalmic imaging

Correspondence to: Robert L. Gendron, Division of BioMedical Sciences, Faculty of Medicine, Memorial University of Newfoundland, 300 Prince Philip Drive, St. John's, NL, A1B 3V6, Canada Phone (709)-864-3359; email: rgendron@mun.ca

can also be used in combination with other retinal imaging techniques in the experimental research setting in rodents and other animals. We now use ophthalmic imaging approaches in developmental biologic and pathobiological studies of the lumpfish eye [2,7].

Although several reports described the use of smartphones to perform ophthalmic imaging in humans [8-16], animals in veterinary medicine [17,18] and experimental animals [19], to our knowledge, there are no reports of adapting smartphone ophthalmic imaging to existing experimental ocular imaging instrumentation. There are also no reports of use of 3D printing technology to improve the efficacy of handheld smartphone-based ophthalmic imaging. Although retinal imaging microscopes exist, their cost can be prohibitive. As basic science research budgets tighten in many countries, 3D printing offers a highly affordable alternative to modify existing instrumentation to expand functional utility. These concepts are important, because ophthalmic imaging approaches, such as SD-OCT, are de rigueur in retinal research laboratories today. The objective of the present study was to explore the use of 3D printing to increase the functionality of existing rodent SD-OCT laboratory equipment and previously described smartphone-based ophthalmic imaging. This was accomplished through the construction of a custom attachment controlled by the highly precise rodent stage of the SD-OCT instrument. The equipment modified was a Leica/Bioptigen (Concord, Canada) Envisu R-Class SD-OCT instrument. Thus, high-quality ophthalmic imaging and additional functions were provided at low cost and ease of production. We also tested a handheld approach using the 3D printed apparatus on lumpfish [2,7].

METHODS

Assessing existing equipment: Our laboratory recently acquired a Leica/Bioptigen Envisu R-Class SD-OCT instrument for the use of preclinical research in mice. This instrument is composed of a rodent stage (mouse or rat), SD-OCT hardware, and a high-precision platform that provides multiple degrees of adjustability. Although this setup is optimized for mouse retinal SD-OCT imaging, its secondary ophthalmic imaging function is not ideal for obtaining publication-quality research images. We proposed that an attachment could be designed and produced to fit the SD-OCT hardware clamp, allowing us to utilize the machine's existing animal stage to take advantage of its high-precision adjustability. To achieve the proper optical setup for the desired capability of ophthalmic imaging, a clear 78 diopter (D) lens was incorporated into the design of the attachment. A sixth-generation Apple (Cupertino, CA) iPod Touch and the FiLMiC (Seattle, WA) Pro app were purchased from Walmart and the Apple App Store, respectively, to be used as an affordable means of capturing high-quality digital images and video, and to simulate how easily the attachment can be used with a personal smartphone.

Measurements of the SD-OCT instrument components and the 78 D lens from Volk Optical (Mentor, OH), were taken using manual calipers to within one tenth of a millimeter. All components were sketched, and measurements were used for the design and modeling process.

Design and modeling: All virtual prototyping was completed using an Apple MacBook Pro running Blender (Amsterdam, Netherlands) Version 2.78. Blender is open-source freeware designed for creating 3D computer graphics with the ability to export projects as stereolithography (STL) files. STL is one of the most common file formats supported by 3D printers and online printing services, and therefore, was the format of choice for exporting the files. Blender was chosen over other 3D modeling software because it is powerful, free to use, and supported by MacOS, Windows, and Linux. The nature of freeware, such as Blender, lends itself to massive online instructional user support in many forms, including user forums and instructional videos. The authors had no previous experience designing with Blender and learned what was required from free online instructional content.

The design and modeling process was iterative, involving printing several prototypes and making refinement modifications to each. The final working model was the third revision of the original and was composed of three pieces. The phone case portion of the apparatus was not designed by the authors but was a free model that was downloaded from the Thingiverse website. Renderings of the separate component models can be seen in Figure 1.

Once the final prototype pieces were mounted to the SD-OCT platform, the lens and the iPod camera were aligned, and pieces of the apparatus were fixed using Super Glue (Ontario, CA). For the sake of focal length adjustability, the piece housing the 78 D lens was fastened using a 0.25 × 1.00 inch bolt and wing nut.

Prototype printing: Our laboratory worked closely with Memorial University's 3D printing team from the Faculty of Medicine for the rapid prototyping portion of this project. This 3D printing facility is a learner-operated laboratory dedicated to supporting biomedical research and medical education and integrating 3D printing technologies in the medical field. The printable pieces of the device were all constructed using an Ultimaker (Cambridge, MA) 2+ 3D printer made available to us by the Memorial University facility. Each piece was

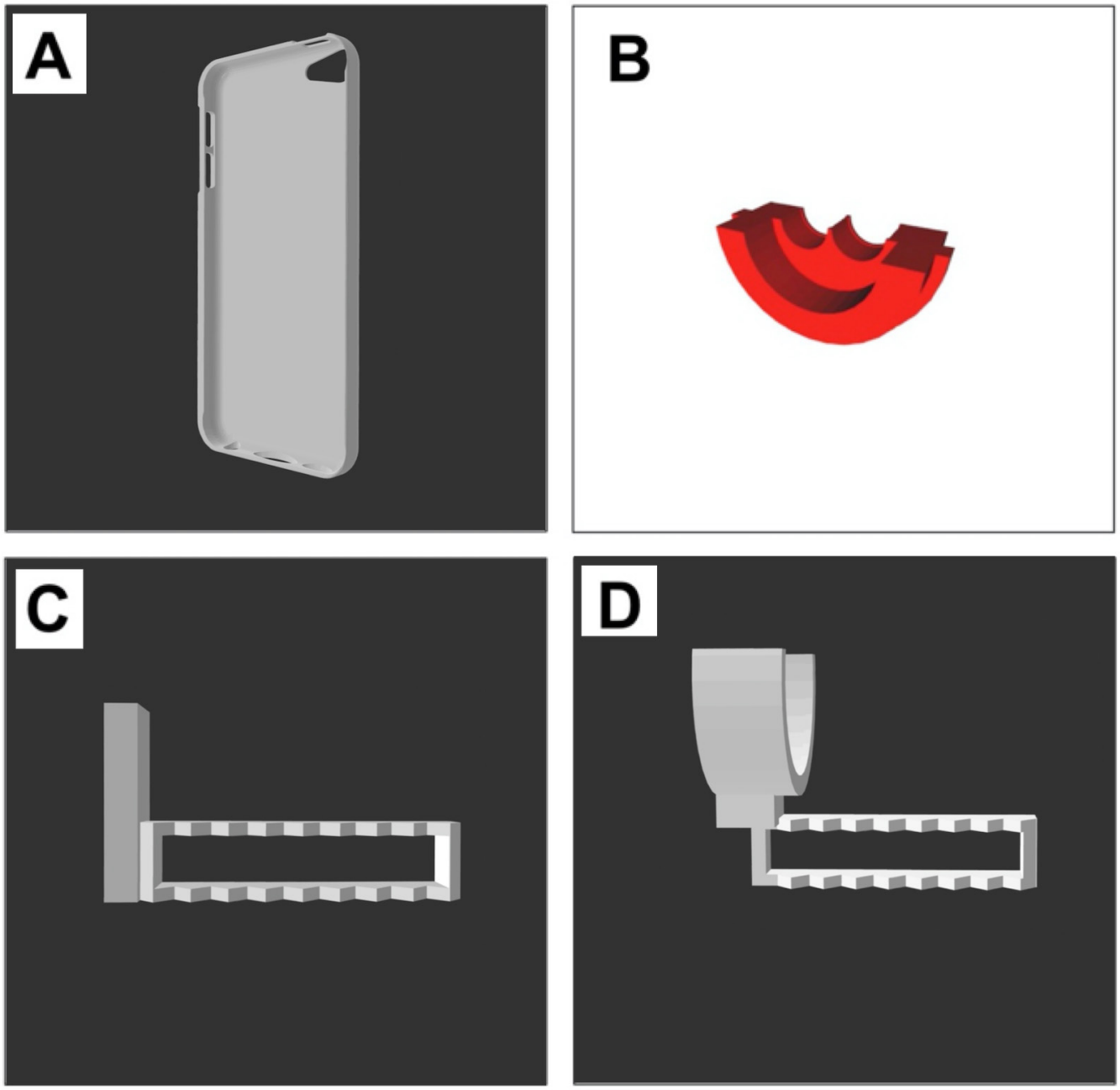

Figure 1. 3D-printed components of the ophthalmic imaging apparatus. **A**: iPod Touch case. **B**: Focal point adjustment slide. **C**, **D**: 78 diopter lens mount.

constructed using polylactic acid filament at a nozzle setting of 0.4 mm. Plastic filament was also provided free of charge by the facility.

The printer configuration and print execution were supported by Memorial University's 3D printing facility. Cura (Geldermalsen, Netherlands) Version 2.5.0 software was used to convert the STL files into G-code. G-code is a numerical control program language read by the printer's hardware. The component that required the most time to print was the iPod case, which ran for 8 h. All other pieces printed within less than 3 h each. All 3D-printed parts of the assembly are shown in Figure 1.

Prototype testing, materials, and cost: Although the prototypes were built in the 3D printing laboratory at Memorial

University's Faculty of Medicine, we realize that not everyone has easy access to such services. An online search for 3D printing services introduced us to 3D Hubs (Amsterdam, Netherlands), a website that operates globally and aims to connect designers with crowd-sourced printers within 10 miles of their locations. This website connected us with a commercial printing company located 17 km from Memorial University. We submitted STL files through 3D Hubs, and the local company provided a quoted price of CAD 18.50 for all three parts with a lead time of 48 h or less. Excluding the SD-OCT instrument and the iPod, the costs of all other components used in this system for obtaining mouse fundus images are listed in Table 1.

Table 1. Cost of ophthalmic imaging apparatus excluding spectral domain optical coherence tomography (SD-OCT) and iPod.

Item	Cost (CAD)
3D Printed Parts	$18.50
78 Diopter Lens	$440.00
Fastening Hardware	$2.00
Total Cost	**$460.50**

3D printed parts are based on a quote from 3D Hubs.

Use of the FiLMiC Pro app: Using the FiLMiC Pro app, the light source of the iPod Touch was set to medium brightness using the FiLMiC Pro app Torch Adjust tool, and an appropriate distance from the lens to the mouse eye was approximated using a piece of white paper marked with an X. The paper position was adjusted until the beam from the light source was condensed on the center of the X. We were also careful to ensure that at this position the view was inverted, and the picture on the iPod was in focus. Once this was achieved, the stage was adjusted in three dimensions such that the mouse's eye would be approximately where the center of the X was. The mouse was then positioned on the stage. The mouse's face was observed directly to appreciate the position of the condensed beam of light with respect to the eye, and adjustments were made so that the beam was directed into the pupil. The iPod mount was then backed away from the mouse's face, and the eye was observed indirectly through the apparatus. The apparatus was advanced toward the mouse's eye in a stepwise fashion, while fine adjustments were made to the mouse's position to keep the condensed light beam shining through the pupil. As the apparatus approached the mouse's eye, a vertical sliver of illuminated retinal tissue came into view. The apparatus was advanced once more to bring the retinal sliver into fine focus. The light source (Torch tool) was adjusted to maximum brightness using the FiLMiC Pro app Torch Adjust window, and the mouse's angular position was adjusted until the entire image displayed retinal tissue. At that time, final minor adjustments were made to the position of the apparatus to maximize the image focus before recording using the FiLMiC Pro app Video Record tool. The torch level was also varied to test effects of different light levels on the fundus image.

Mouse ophthalmic imaging: Healthy C57BL/6 mice (Jackson Laboratory, Bar Harbor ME) were lightly anesthetized with 100 mg/kg ketamine per 10 mg/kg xylazine for ophthalmic imaging. Anesthetized mice were administered a drop of tropicamide into each eye after which each eye was then treated with Tear-Gel ophthalmologic lubricating gel (Alcon, Mississauga ON, Canada). The mice were then wrapped in a Kimwipe (Fisher Scientific, Ottawa ON, Canada) and mounted into the mouse cradle of the SD-OCT instrument with a 4 × 4 inch piece of gauze folded four times placed under the front of the mouse's body and head area (Figure 2A). The magnetic bite bar assembly of the mouse cradle was removed from the fixed black metal base. The camera distance was set at 22–28 mm, the mouse was positioned with the cradle at a 45 degree angle, and the mouse's nose was aligned with the fixed black metal base bar for the removable bite bar assembly. The mouse was gently secured in place using medical tape and a Kimwipe (Figure 2A).

Lumpfish ophthalmic imaging: Young adult lumpfish of approximately 1 year of age, housed at the Dr. Joe Brown Aquatic Research Building, Department of Ocean Sciences, Memorial University, were imaged without anesthesia at tank side by having one person remove the fish from the water and gently restrain the fish while another person aimed the imaging device toward the fish's eye for image capture. Fish fundus and ophthalmoscopic imaging took only a few moments, after which the fish were returned to their tanks. Mouse and lumpfish work was approved by the Institutional Animal Care Committee of Memorial University. The study adhered to the ARVO Statement for Use of Animals in Research

RESULTS

After the SD-OCT bore lens and camera were removed, the fully assembled 3D-printed ophthalmic imaging smartphone system was mounted quickly and easily to the Leica/Bioptigen Envisu R-Class SD-OCT instrument (Figure 2A). The original equipment manufacturer (OEM) bore lens and camera cradle movement component had to be positioned some distance closer to the mouse cradle than that used for SD-OCT, but this shift in position was easily performed with the bore lens and camera adjustment wheel. When positioned

and clamped into place, the control screen of the 3D-printed fundus smartphone system was easily visible, accessible, and controllable (Figure 2B). Thus, the objectives for the apparatus fit, ease of mounting, and stability on the SD-OCT stage were met.

As the apparatus approached the mouse's eye, a vertical sliver of illuminated retinal tissue came into view. As the apparatus was advanced further, the retinal sliver was brought into fine focus. After the light source (Torch tool) was adjusted to maximum brightness using the FiLMiC Pro app Torch Adjust window, and the mouse's angular position was adjusted, the entire image displayed retinal tissue. Final minor adjustments made to the position of the apparatus to maximize the image focus optimized the recording using the FiLMiC Pro app Video Record tool. Varying of the torch level to effect different light levels also was effective at optimizing

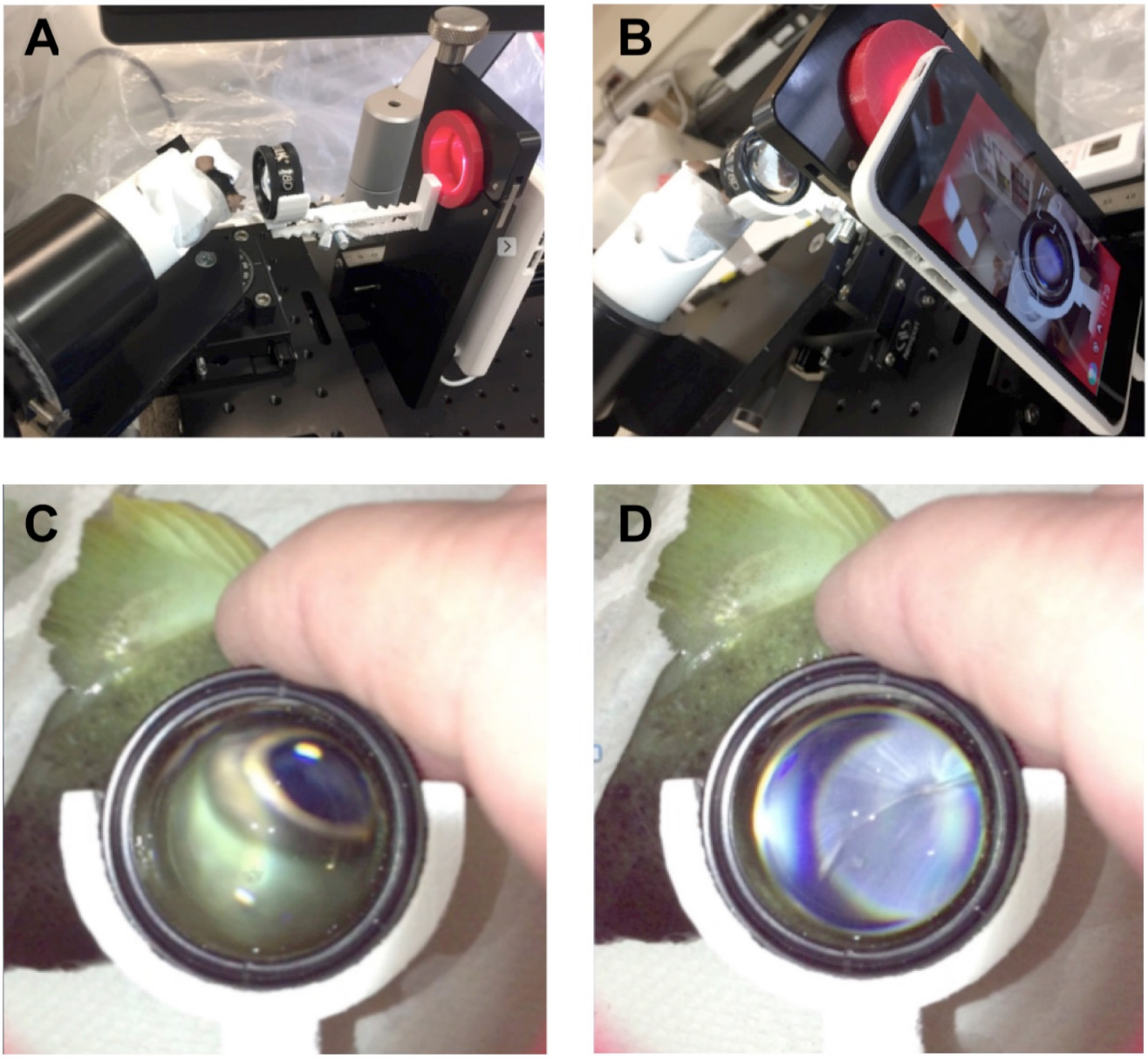

Figure 2. Ophthalmic imaging apparatus setup using mice and lumpfish. **A**: Mouse on the Bioptigen spectral domain optical coherence tomography (SD-OCT) rodent stage showing the positions of the three-dimensional (3D)-printed parts and the 78 diopter (D) lens. **B**: FiLMiC Pro imaging of mouse fundus on an iPod screen. **C**: Ocular structures of lumpfish being imaged manually at tank side. **D**: FiLMiC Pro imaging of lumpfish fundus on an iPod screen.

the fundus image observed. Thus, the objectives for taking advantage of the image adjustment features of the FiLMiC Pro app were met.

Clear digital high-definition (HD) video images of the live mouse fundus were captured in FiLMiC Pro with the 3D-printed fundus smartphone system mounted on the SD-OCT instrument (Figure 3). Blood vessel colors of red versus blue could be clearly discerned. High torch settings seemed to allow better imaging of the retinal blood vessels, while the medium torch setting seemed to allow better imaging of the optic disc. Lumpfish were easily and rapidly imaged at tank side (Figure 2C,D show FiLMiC Pro imaging of lumpfish fundus on the iPod screen), and as we have reported previously using the apparatus ([2,7]. Thus, the objectives for using the new apparatus for rapidly obtaining high-resolution ophthalmic images were met.

DISCUSSION

The literature contains several reports of the use of smartphones to perform ophthalmic imaging in humans with comparisons to conventional fundus photography indicating that smartphone ophthalmic imaging can be an effective substitute [8-16]. Smartphone ophthalmic imaging has also been described in several animals in a veterinary medicine setting [17,18] and in experimental animals in a research laboratory setting [19]. We are investigating the eyes of lumpfish, have successfully performed SD-OCT on these animals, and have used prototypes of the apparatus described in this report for ophthalmic imaging in lumpfish [2]. However, to our knowledge, there are no other reports of any type of high-resolution ophthalmic imaging of marine teleosts. Therefore, the apparatus we describe in this report advances the field by providing a methodological approach for ophthalmic imaging of marine teleosts.

Several previous studies described affordable adaptations to improve the use of smartphones in ophthalmic imaging [22,23]. Custom-built cradles or devices, some involving the use of 3D printing, for optimizing human smartphone-based fundus photography have been described [24]. Smartphone-based fluorescein angiography has also been described [25]. All of these previous studies validated the use of smartphones in ophthalmic imaging. However, without proper holding stages, smartphones are difficult to use on small animals. The assembly described, as adapted to the rodent stage of an existing SD-OCT instrument, or used in a handheld manner, advances the state of the technology of smartphone ophthalmic imaging by further optimizing efficacy and by taking advantage of the stability and precise adjustability of the OCT instrument stage to facilitate clear digital true-to-life color HD video images of live small animal fundus. With the apparatus used in conjunction with the Leica/Bioptigen Envisu R-Class SD-OCT instrument, it is now possible to perform SD-OCT and high-resolution ophthalmic imaging in one rapid session, thus obtaining more information from the experimental animal in less time and with less stress to the animal. The ability to distinguish the integrity and

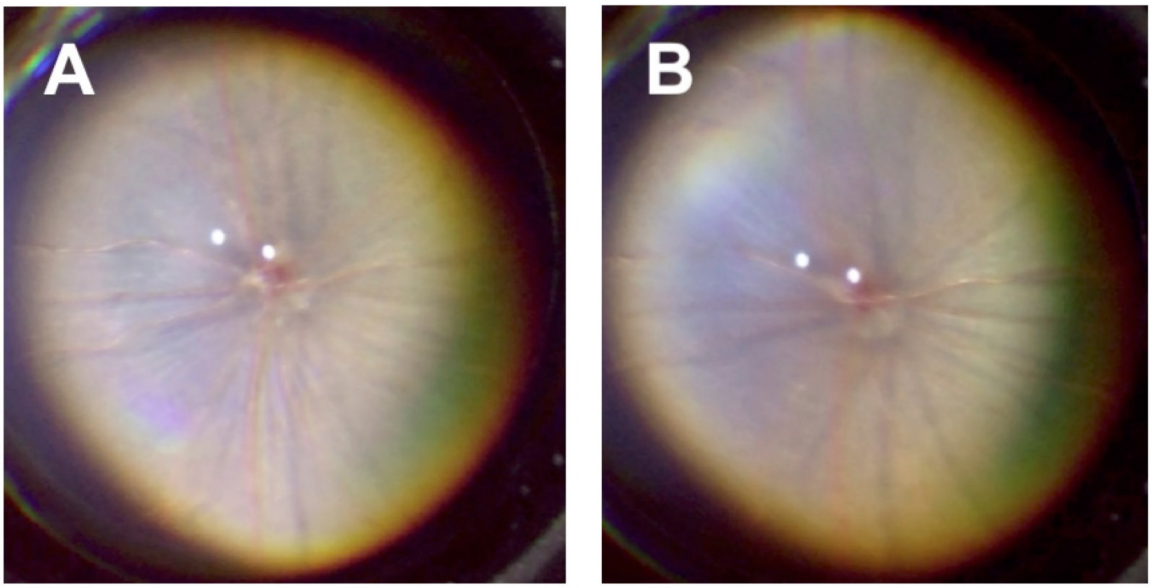

Figure 3. FiLMiC Pro images of mouse fundus from an iPod screen recorded with apparatus fixed to the Bioptigen rodent stage at two light levels. **A**: High torch setting. **B**: Medium torch setting.

actual colors of retinal blood vessels and the optic disc could be useful for studies of inner retinal vasculature and optic nerve head in rodent research. Similarly, the rapid handheld approach for ophthalmic imaging at tank side afforded by this apparatus can advance research using cultured marine teleosts as model organisms [2,7]. In this setting, even fine details of the inner retinal surface can be visualized and video-recorded in the field within seconds. Using this technique, we observed distinct radial lines on the inner retinal surface of live lumpfish and used the apparatus to record video of anterior ocular pathology ([2,7]; Figure 2). Although we have not yet identified the radial inner retinal lines, they cannot be accounted for by inner retinal vasculature which is limited in lumpfish [2]. We speculate that the lines might represent either large radial columns associated with Müller cells or myelinated bundles of retinal ganglion cell axons, both of which are known to exist in deep sea teleosts [26] but have not yet, to our knowledge, been imaged using ophthalmoscopy approaches. As lumpfish frequent deep water [27-30], it is conceivable that they might have evolved variations of these structures. Alternatively, the apparatus could be used for marine teleost ophthalmic imaging on the SD-OCT stage, provided that the size of the animal is amenable to fitting on the instrument stage. We have adapted other readily available materials, such as modified commercially available residential silicone soap dishes, to create cradles that are waterproof, flexible, and appropriately sized for juvenile or young adult marine teleosts such as lumpfish. The STL files for producing the apparatus described in this report are available upon request.

ACKNOWLEDGMENTS

This work was supported in part by a Summer Undergraduate Research Award (SURA) from Memorial University Faculty of Medicine to JM. Infrastructure funding from Canada Foundation for Innovation (CFI) enabled acquisition of the Leica/Bioptigen Envisu R-Class SD-OCT instrument. Animal work was supported by a Vitamin Research Fund award from Ocean Frontier Institute and Memorial University Faculty of Medicine Dean Awards to RLG and HP. We thank Danny Boyce, Jennifer Monk and Jessica Fry of the Dr. Joe Brown Aquatic Research Building of Department of Ocean Sciences, Memorial University. We thank Memorial University Engineering work term student Amy Feltham who was employed for the summer of 2017 by Memorial University 3D printing facility of the Faculty of Medicine. We thank the reviewers of the manuscript for helpful and constructive comments that have improved the quality of the manuscript.

REFERENCES

1. Fox JG. The Mouse In Biomedical Research. Amsterdam: Academic Press. 2007.

2. Ahmad R, Paradis H, Boyce D, McDonald J, Gendron RL. Novel characteristics of the cultured Lumpfish Cyclopterus lumpus eye during post-hatch larval and juvenile developmental sages. J Fish Biol 2019; 94:297-312. [PMID: 30565257].

3. Toms M, Tracey-White D, Muhundhakumar D, Sprogyte L, Dubis AM, Moosajee M. Spectral Domain Optical Coherence Tomography: An In Vivo Imaging Protocol for Assessing Retinal Morphology in Adult Zebrafish. Zebrafish 2017; 14:118-25. [PMID: 28051361].

4. Bailey TJ, Davis DH, Vance JE, Hyde DR. Spectral-domain optical coherence tomography as a noninvasive method to assess damaged and regenerating adult zebrafish retinas. Invest Ophthalmol Vis Sci 2012; 53:3126-38. [PMID: 22499984].

5. Collery RF, Veth KN, Dubis AM, Carroll J, Link BA. Rapid, accurate, and non-invasive measurement of zebrafish axial length and other eye dimensions using SD-OCT allows longitudinal analysis of myopia and emmetropization. PLoS One 2014; 9:e110699-[PMID: 25334040].

6. Rayna T, Striukova L. From Rapid Prototyping To Home Fabrication: How 3D Printing Is Changing Business Model Innovation. Technol Forecast Soc Change 2016; 102:214-24. .

7. Paradis H, Ahmad R, McDonald J, Boyce D, Gendron RL. Ocular tissue changes associated with anterior segment opacity in lumpfish (Cyclopterus lumpus L) eye. J Fish Dis 2019; 42:1401-8. [PMID: 31393016].

8. Nazari Khanamiri H, Nakatsuka A, El-Annan J. Smartphone Fundus Photography. J Vis Exp 2017; 125:55958-[PMID: 28715396].

9. Muiesan ML, Salvetti M, Paini A, Riviera M, Pintossi C, Bertacchini F, Colonetti E, Agabiti-Rosei C, Poli M, Semeraro F, Agabiti-Rosei E, Russo A. Ocular fundus photography with a smartphone device in acute hypertension. J Hypertens 2017; 35:1660-5. [PMID: 28306635].

10. Toy BC, Myung DJ, He L, Pan CK, Chang RT, Polkinhorne A, Merrell D, Foster D, Blumenkranz MS. Smartphone-based dilated fundus photography and near visual acuity testing as inexpensive screening tools to detect referral warranted diabetic eye disease. Retina 2016; 36:1000-8. [PMID: 26807627].

11. Bolster NM, Giardini ME, Bastawrous A. The Diabetic Retinopathy Screening Workflow: Potential for Smartphone Imaging. J Diabetes Sci Technol 2015; 10:318-24. [PMID: 26596630].

12. Ryan ME, Rajalakshmi R, Prathiba V, Anjana RM, Ranjani H, Narayan KM, Olsen TW, Mohan V, Ward LA, Lynn MJ, Hendrick AM. Comparison Among Methods of Retinopathy Assessment (CAMRA) Study: Smartphone, Nonmydriatic,

and Mydriatic Photography. Ophthalmology 2015; 122:2038-43. [PMID: 26189190].

13. Adam MK, Brady CJ, Flowers AM, Juhn AT, Hsu J, Garg SJ, Murchison AP, Spirn MJ. Quality and Diagnostic Utility of Mydriatic Smartphone Photography: The Smartphone Ophthalmoscopy Reliability Trial. Ophthalmic Surg Lasers Imaging Retina 2015; 46:631-7. [PMID: 26114843].

14. Darma S, Zantvoord F, Verbraak FD. The quality and usability of smartphone and hand-held fundus photography, compared to standard fundus photography. Acta Ophthalmol 2015; 93:e310-1. [PMID: 25529489].

15. Russo A, Morescalchi F, Costagliola C, Delcassi L, Semeraro F. A Novel Device to Exploit the Smartphone Camera for Fundus Photography. J Ophthalmol 2015; 2015:823139-[PMID: 26137320].

16. Maamari RN, Keenan JD, Fletcher DA, Margolis TP. A mobile phone-based retinal camera for portable wide field imaging. Br J Ophthalmol 2014; 98:438-41. [PMID: 24344230].

17. Kanemaki N, Inaniwa M, Terakado K, Kawarai S, Ichikawa Y. Fundus photography with a smartphone in indirect ophthalmoscopy in dogs and cats. Vet Ophthalmol 2017; 20:280-4. [PMID: 27302683].

18. Balland O, Russo A, Isard PF, Mathieson I, Semeraro F, Dulaurent T. Assessment of a smartphone-based camera for fundus imaging in animals. Vet Ophthalmol 2017; 20:89-94. [PMID: 26775579].

19. Haddock LJ, Kim DY, Mukai S. Simple, inexpensive technique for high-quality smartphone fundus photography in human and animal eyes. J Ophthalmol 2013; 2013:518479-[PMID: 24171108].

20. Raju B, Raju NS, Akkara JD, Pathengay A. Do it yourself smartphone fundus camera - DIYretCAM. Indian J Ophthalmol 2016; 64:663-7. [PMID: 27853015].

21. Micheletti JM, Hendrick AM, Khan FN, Ziemer DC, Pasquel FJ. Current and Next Generation Portable Screening Devices for Diabetic Retinopathy. J Diabetes Sci Technol 2016; 10:295-300. [PMID: 26888973].

22. Sharma A, Subramaniam SD, Ramachandran KI, Lakshmikanthan C, Krishna S, Sundaramoorthy SK. Smartphone-based fundus camera device (MII Ret Cam) and technique with ability to image peripheral retina. Eur J Ophthalmol 2016; 26:142-4. [PMID: 26350993].

23. Shanmugam PM, Mishra D, Ramanjulu R. Fluorescein fundus angiography using a smartphone. Retina 2014; 34:e6-7. [PMID: 24553349].

24. Collin SP, Lloyd DJ, Wagner HJ. Foveate vision in deep-sea teleosts: a comparison of primary visual and olfactory inputs. Philos Trans R Soc Lond B Biol Sci 2000; 355:1315-20. [PMID: 11079422].

25. Davenport J. Synopsis of biological data on the lumpsucker cyclopterus lumpus (Linnaeus, 1758). FAO Fish Synop 1985; 14731-.

26. Blacker RW. Pelagic records of the lumpsucker, Cyclopterus lumpus L. J Fish Biol 1983; 23:405-17. .

27. Rosen S, Holst JC. DeepVision in-trawl imaging: sampling the water column in four dimensions. Fish Res 2013; 148:64-73. .

28. Kennedy J, Jónsson SP, Ólafsson HG, Kasper JM. Observations of vertical movements and depth distribution of migrating female lumpfish (*Cyclopterus lumpus*) in Iceland from data storage tags and trawl surveys ICES J Mar Sci 2016; 73:1160-9. .

Articles are provided courtesy of Emory University and the Zhongshan Ophthalmic Center, Sun Yat-sen University, P.R. China. The print version of this article was created on 31 March 2021. This reflects all typographical corrections and errata to the article through that date. Details of any changes may be found in the online version of the article.